B. Electrochem 4(8) August 1988, pp 723-728

HIGH PERFORMANCE POROUS GAS DIFFUSION ELECTRODES FOR OXYGEN REDUCTION IN ALKALINE FUEL CELLS

R CHANDRASEKARAN, I ARULRAJ, R PATTABIRAMAN, S DHEENADAYALAN, S MUZHUMATHI and V K VENKATESAN
Central Electrochemical Research Institute, Karaikudi-623 006, INDIA
[Received: 1988 January; Accepted in revised form: 1988 June]

Porous gas diffusion electrodes of two layer and three layer type are prepared by cold compacting and sintering technique. The optimum concentration of acetylene black is 2 wt% and activated charcoal is 10 wt%. The incorporation of silver by different techniques like thermal decomposition of silver salts is presented. The amount of silver varies from 53 mg.cm^{-2} to 106 mg.cm^{-2}. Electrode area is 30 cm^2. The electrodes were polarised as oxygen gas diffusion electrodes in 6.0 M KOH solution at 333K.The electrodes were found to be polarised to -145 mV at 60 mA.cm^{-2} and to -190 mV at 80 mA.cm^{-2} at 333K. These electrodes have been tested continuously and were found to show the same performance for 500 hrs -1000 hrs

The performance of the same was compared with the electrode containing acetylene black, heat treated and untreated in nitrogen atmosphere at 1073K for 20 hours. Incorporation of platinised acetylene black (carbon) as electrocatalyst for oxygen reduction has also been attempted.

Key words: Gas diffusion, porous electrodes, electrocatalysis

INTRODUCTION

The reduction of oxygen is the most important cathodic reaction in fuel cells and metal-air batteries. In the near future, oxygen electrodes may be used in brine electrolysis [1]. The sintered porous nickel electrodes employ non-noble metal catalysts like cobalt aluminate [2], perovskites [3] and silver or silver-based catalysts [4]. In earlier communications, the results of the polarisation behaviour of oxygen gas diffusion electrodes employing activated charcoal [5], acetylene black [6] or silver formed insitu from silver carbonate [7] or silver on alumina [8] were reported.

The long term performance of cathodes containing silver catalysts in alkaline medium are presented here. Activated charcoal and silver dispersed on skeletal nickel matrix have also been studied. Charges in the performance of the porous electrodes due to flooding, loss of surface area or catalytic activity and their effect on the electrode performance is studied by the AC impedance method [9,10]. A general model of the oxygen reduction kinetics in porous electrodes is proposed.

EXPERIMENTAL

The different catalysts, namely silver formed insitu from silver carbonate or activated charcoal or combination of both, have been used as electrode catalyst. Coconut shell charcoal activated in ammonia and carbon dioxide atmospheres alternatively at 1273K for 100 hours has been employed. The preparation of the silver-based catalyst is the same as reported earlier [6]. Three layer electrodes of area 30 cm ^{2} were prepared by the procedure described earlier [5]. The steady state galvanostatic polarisation studies have been carried out in 6N KOH at various temperatures by employing an alkaline mercuric oxide reference electrode [11]. The porosity and pore size distribution curves were obtained by Mercury Penetration Porosimeter. SEM characterisation of the electrodes were done with Scanning Electron Microscope.

RESULTS AND DISCUSSION

The characteristics of the electrocatalysts and electrodes employed in these studies are given in Table 1. Figs. 1a, 1b, 1c and 1d show the SEM photographs of the porous oxygen gas diffusion electrode containing activated charcoal and silver (Electrode 3). Fig. 1a shows the vertical cross section of the electrode with clear distinction of the three layers, the middle layer containing the catalyst and the three layers differing in pore diameters. The thickness of each layer is found to be fairly uniform throughout the whole electrode area. Fig. 1b shows the SEM photograph of the catalyst layer (middle layer). Figs. 1c and 1d show the EPMA spectrum of silver and nickel respectively in the middle layer which confirm the uniform distribution of silver and nickel in the catalyst layer. Figs. 2a, 2b and 2c show the SEM photograph of the oxygen electrode containing only silver (Electrode 5).

TABLE-I: Characteristics of oxygen electrodes

Electrode No.	Electrocatalyst in the catalyst layer	Electrocatalyst amount: mg.cm^{-2}
1	Activated charcoal	38
2	Activated charcoal + silver insitu from Ag_2CO_3,	38 + 26
3	Activated charcoal + silver insitu from Ag_2CO_3	38 + 52
4	Activated charcoal + silver insitu from Ag_2CO_3	38 + 52
5	Silver insitu from silver carbonate	76
6	Silver insitu from silver carbonate	104

Fig.3 and 4 show the pore volume and pore size distribution curves of the electrodes 1,3 and 5 respectively. From Fig.4, we can infer that the distribution curves show two maxima corres-

0256-1654/88/$ 3-50/

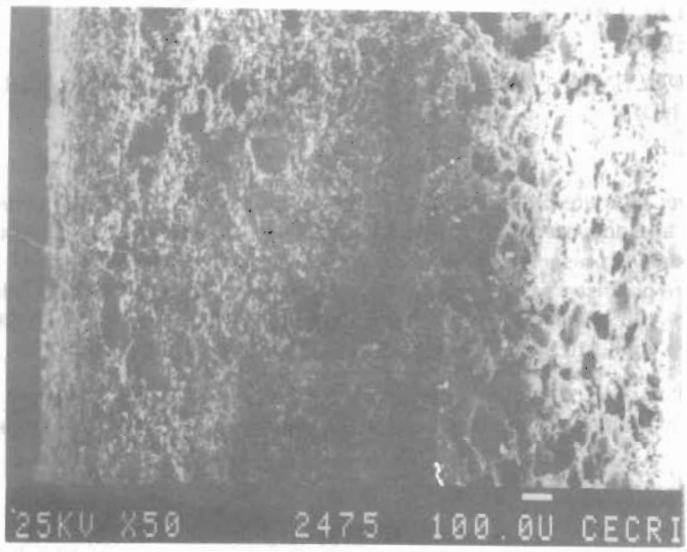

Fig.1: SEM micrograph of porous oxygen gas diffusion electrode 3. (a) SEM photograph of the electrode in vertical cross section

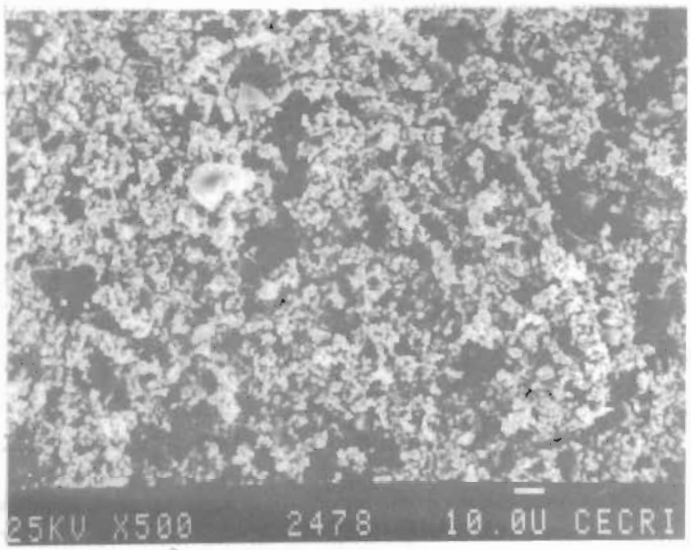

(b) SEM photograph of the middle layer

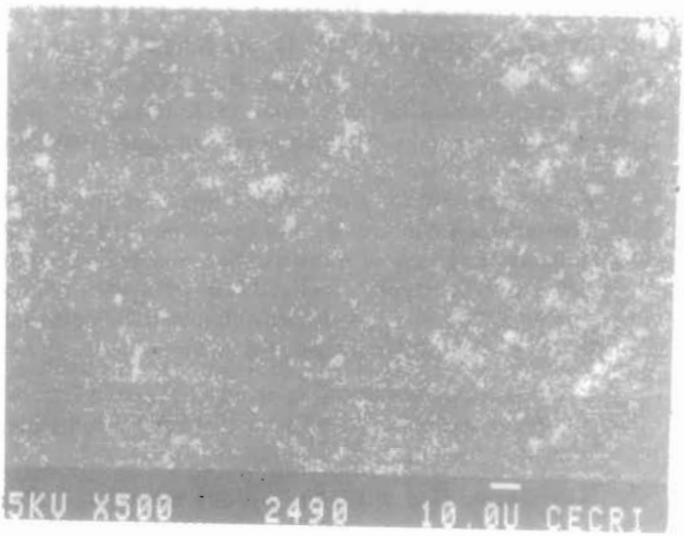

(c) EPMA spectrum of silver in the middle layer

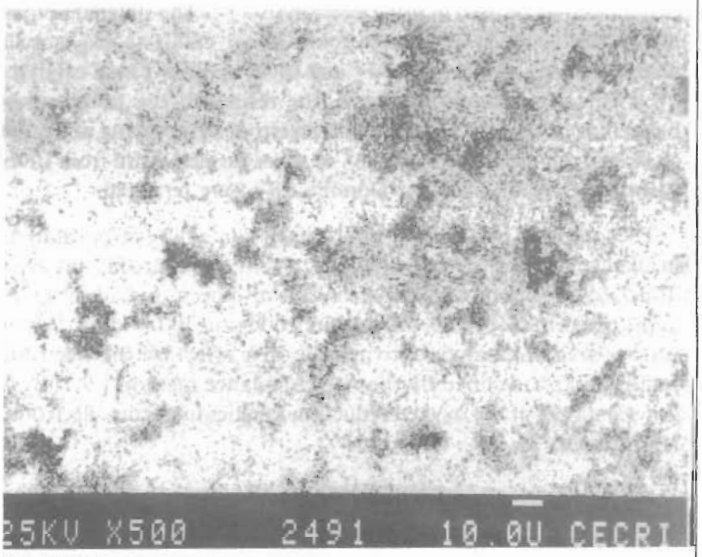

(d) EPMA spectrum of nickel in the middle layer

ponding to pore dia 6 μm and 0.7 μm respectively for the electrode 3 and 5 (curve 3 and 2 respectively). The pores in the lower range is mainly due to the pores formed by the supporting nickel matrix in the operating and catalyst layers. This is about 25% of the total porosity of the electrodes whereas the other maxima correspond to the pores formed between the nickel and the catalyst. This is fairly widely distributed to the extent of 50 to 55% in the pore dia range 2 to 10 μm. This increase is not observed in the case of electrode 1 which contains only activated charcoal. The silver carbonate during thermal decomposition thus creates pores to a greater extent in the other electrodes (Electrode 3 and 5) leaving behind high surface area catalyst in the electrode.

Steady state polarisation studies

Fig.5 shows the steady state galvanostatic polarisation curves for the various oxygen electrodes (Nos. 1 to 6) for oxygen reduction in 6N KOH at 333K and p O_2 = 1.0 kg. cm^{-2}. The polarization of the electrodes at 80-120 $mA.cm^{-2}$ were compared. The electrode containing only activated charcoal as the catalyst (Electrode 1) was found to show a current density of 80 $mA.cm^{-2}$ (curve 1) at -300 mV vs Hg/HgO/OH. . The performance of the above electrodes was found to increase with silver addition in the catalyst layer (curves 2,3 and 4). Current densities of the order of 100 mA. cm^{-2} and

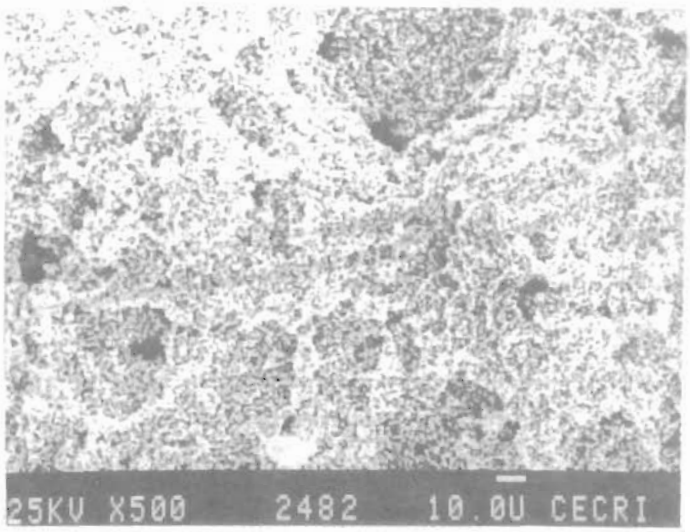

Fig.2: SEM micrograph of porous oxygen gas diffusion electrode 5. (a) SEM photograph of the middle layer

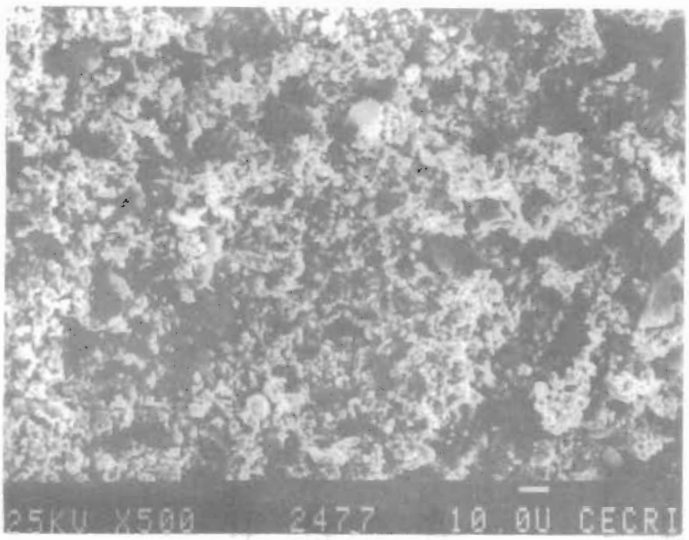

(c) SEM photograph of the gas layer

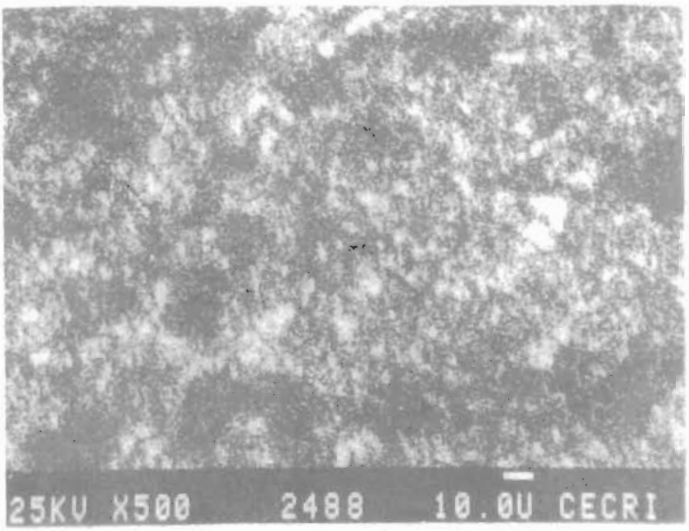

(b) EPMA spectrum of silver in the middle layer

120 mA.cm^{-2} were obtained at silver amounts of 26 mg.cm^{-2} and 52 mg.cm^{-2} respectively at -300 mV. The polarisation of the electrodes containing activated charcoal and silver for different batches of electrodes (Electrode 3 and 4) was found to be the same and their long term performance was also found to be same.

The electrodes containing silver alone as the catalyst performed well and current densities beyond 160 mA.cm^{-2} can be obtained at -300 mV vs Hg/HgO (curves 5 and 6 in Fig.5). The electrodes were also subjected to continuous polarisation studies. The polarisation was found to be the same even after 1000 hours of testing. Fig.6 shows the galvanostatic polarisation curves for electrode 6

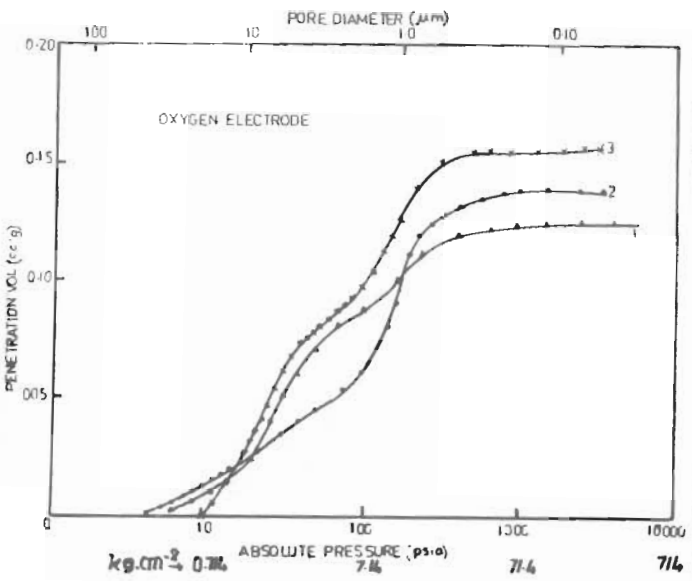

Fig.3: Pore-volume-mercury penetration curve for the porous oxygen gas diffusion electrodes. (1) Electrode 1; (2) Electrode 5; and (3) Electrode 3.

at different temperatures. (Curves 1 to 3 at 303K, 333K and 353K respectively for electrodes 6 and curve 4 at 353K for electrode 2). For practical considerations current densities upto a polarisation

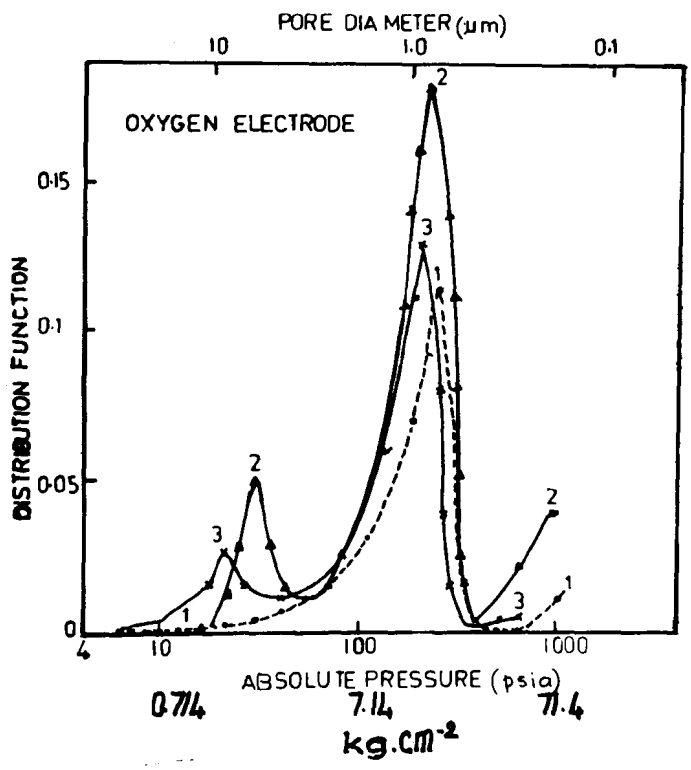

Fig.4: Pore size distribution curves for oxygen electrodes (1) Electrode 1; (2) Electrode 5; and (3) Electrode 3

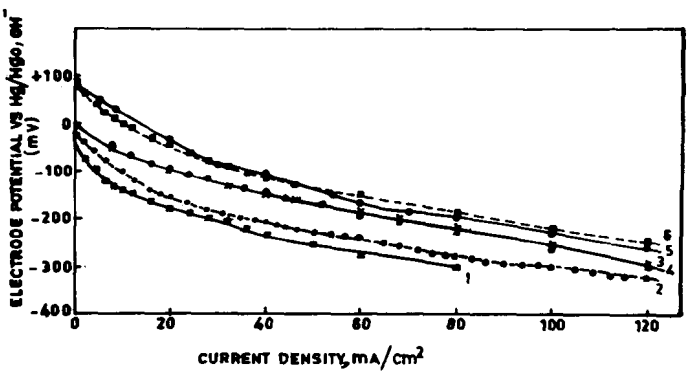

Fig.5: Steady state galvanostatic polarisation curves for the oxygen electrodes in 6.0 M KOH at 333K. Curves nos. correspond to electrode nos.

of - 200mV are found to be important. The polarisation values obtained at different temperatures for all the electrodes studied are given in Table II. The practical current density at -200mV for the electrodes containing only silver was higher than that containing activated charcoal and silver.

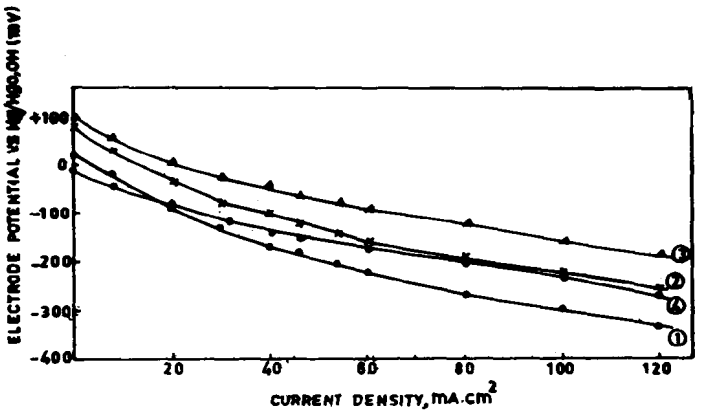

Fig.6: Steady state galvanostatic polarization curves for oxygen reduction at various temperatures. Curves 1 to 3 at 303K, 333K and 353K respectively for electrode 6. Curve 4 at 353K for electrode 2.

TABLE-II: Polarisation data of different oxygen electrodes

Electrode	Current density mA.cm^{-2}	Electrode potentials mV vs Hg/HgO		
		303K	333K	353K
1	40	-280	-230	-
	60	-	-270	-
	80	-	-300	-
2	40	-265	-210	-150
	60	-315	-245	-200
	80	-355	-275	-240
3, 4	40	-210	-145	-105
	60	-255	-185	-145
	80	-300	-220	-190
	120	-380	-295	-245
5	40	-200	-120	-45
	60	-250	-160	-100
	80	-305	-190	-135
	120	-	-260	-190
	160	-	-305	-240
	200	-	-360	-295
6	40	-165	-105	-40
	60	-225	-155	-100
	80	-270	-185	-130
	120	-340	-250	-180
	160	-	-290	-230
	200	-	-345	-270

Impedance measurements and its analysis for oxygen reduction on porous nickel electrodes

The impedance values were measured in the frequency range 10kHz to 0.001 Hz. The impedance values were measured at various electrode potentials e.g. +20 mV (OCP), 0 mV, -25mV, -50mV and -100mV vs Hg/HgO (held potentiostatically). The solution resistance, R_s, determined as the high frequency intercept on the real impedance axis was calculated. R_s values were subtracted from the total impedance [12]. The frequency dispersion gradually approaches a semicircle with increase in cathodic overvoltage where Z'' and Z' represent the imaginary and real components of the cell impedence (Fig.7). At low overpotentials there is a

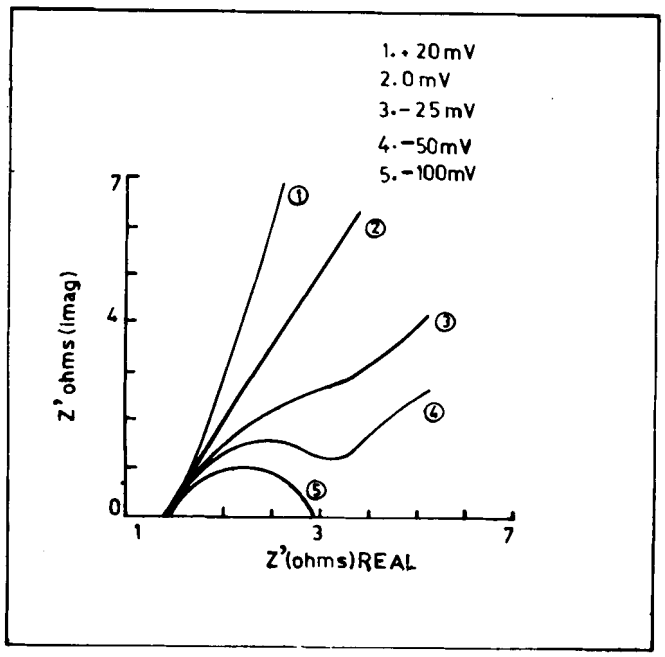

Fig. 7: Faradaic impedance of a porous nickel electrode for oxygen reduction at different O/C potentials. Oxygen gas pressure: 1.0 kg/cm²; Electrolyte: 6M KOH; Temperature 303 K; (1) + 20mV; (2) 0; (3) -25 mV; (4) -50 mV and (5) -100 mV vs Hg/HgO

phase shift of 45° between current and potential. This type of dependence indicates that charge transfer is controlled by diffusion. At high overpotentials, charge transfer takes precedence over diffusion. The diffusion contribution can arise due to the diffusion of oxygen to the reaction site. Such behaviour was also reported for oxygen evolution on nickel [13].

We can construct the equivalent circuit (Fig.8) for oxygen reduction in a similar way [14, 15]. One of the components, Z_{diff} , is rate-controlling at low overpotentials and Z_{kin} at high overpotentials. To understand and evaluate the kinetic parameters, the impedance arising due to the following steps [16] are to be considered as elements in the Faradaic impedance:

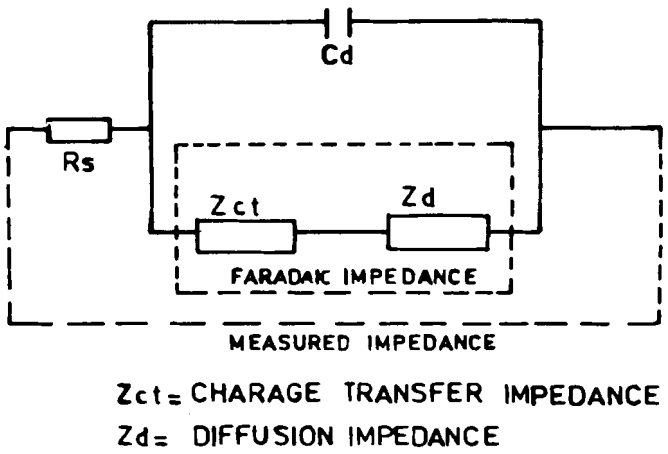

Fig. 8: Equivalent circuit for oxygen reduction reaction on porous electrodes

(i) Oxygen diffusion through the gas phase in the pores

(ii) Oxygen diffusion across the electrolyte film on the active surface to the reaction site

(iii) Adsorption or surface reaction of the oxygen molecule

(iv) Charge transfer i.e. reduction to hydrogen peroxide or water

(v) Diffusion of the reaction product into the electrolyte and diffusion of further reactants etc.

The actual kinetic parameters of the elements are to be correlated with the impedance elements. The typical properties which may affect the measured impedance are being evaluated [17,18].

The double layer capacity was calculated in each case as the intercept on the $(Z\omega)^{-1}_{imag}$ axis as $\omega \longrightarrow \infty$ in the admittance plot, $(Z\omega)^{-1}_{imag}$ vs $(Z\omega)^{-1}_{real}$. This value was almost the same (about 2×10^5 uF) for the porous nickel electrode at all overpotentials. Assuming the double layer capacity for the porous nickel electrode as 14 μ F.cm^{-2} [19], the real surface area was calculated to be 1.5×10^4 cm^2 or the roughness factor is 500 with internal area 1.43×10^3cm^2. g^{-1}. This represents the actual area of the thin wetted film or the electrochemically active surface area. The exchange current density value calculated for this true area is of the order of 10^{-4} A. cm^{-2}. Obviously two electron path way predominates, i.e. the reaction through peroxide formation step, in porous nickel electrodes.

Further elucidation of the i_o value in presence of the catalysts like silver and activated charcoal and the determination of the reaction zone and utilisation of the catalyst etc. will be reported in due course.

REFERENCES

1. E Yeager and P Bindra, *Chem Eng Tech,* **52** (1980) 384

2. K V Kordesh, *Carbon Air Electrodes for Low Temperature Fuel Cells,* Fuel Cell Symposium, ACS Meeting, Atlanta, NJ, 1965

3. A C C Tseung and H L Bevan, *J Electronal Chem,* **45** (1973) 429

4. M W Ranney, *Fuel Cells-Recent Developments,* NDC, New Jersey, USA (1969) p 128

5. R Pattabiraman, R Chandrasekaran, S Muzhumathi, I Arul Raj, S Dheenadayalan and V K Venkatesan, *Trans SAEST,* **22** (1987) 25

6. Indian Patent 143695 (1976)

7.a. R Pattabiraman, R Chandrasekaran, A R Manickam and V K Venkatesan, *Proc Symp Advances in Electrochemical Energy Storage and Conversion,* CECRI, Karaikudi, India (1983) Paper No. 3.2

b. I Arul Raj, S S Amrit Phale, A R Manickam, K Muthu, R Chandrasekaran, C J Indira, R Pattabiraman, K Venkateswara Rao and V K Venkatesan, *Trans SAEST,* **18** (1983) 207

8. K S A Gnanasekaran, R Chandrasekaran, V K Venkatesan and H V K Udupa, *Proc Third National Conference on Power Sources* SAEST (India), (1979) p 119

9. R Holze and W Vielstich in *Advances in Battery Materials and Processes,* Ed J Mc Breen, D T Chin, R S Yeo and A C C Tseung, Princeton (1984) p 230

10. R Holze and W Vielstich, *J Electrochem Soc,* **131** (1984) 2298

11. R Chandrasekaran, T R Jayaraman, C J Indira, R Pattabiraman, K S A Gnanasekaran, V K Venkatesan and H V K Udupa, *Proc Second National Conference on Power Sources* SAEST (India) (1977) p 27

12. W H Smyryl, *J Electrochem Soc,* **132** (1985) 1555

13. T Osala and Y Yatsuda, *Electrochim Acta,* **29** (1984) 677

14. A A Pilla, *J Electrochem Soc,* **117** (1970) 467

15. R Holze, I Vogel and W Vielstich, *Electroanal Chem,* **210** (1986) 277

16. P Drossbach, *Electrochim Acta,* **11** (1966) 667; *ibid* **13** (1968) 2089

17. R de Levie, *Electrochim Acta,* **8** (1963) 751; *ibid,* **9** (1964) 1231

18. S K Rangarajan,*J Electroanal Chem,* **22** (1969) 89

19. J P Candy, P Fouillous, M Keddam and H Takenouti, *Electrochim Acta,* **26** (1981) 1029